

# Magnon-like interactions in a Bose-Einstein condensate: from two-body bound states to mediated superfluidity

Moroni Santiago-García<sup>1</sup> and Arturo Camacho-Guardian<sup>2</sup>

<sup>1</sup>*Instituto Nacional de Astrofísica, Óptica y Electrónica,  
Calle Luis Enrique Erro No.1 Santa María Tonantzintla, Puebla CP 72840, Mexico*

<sup>2</sup>*Instituto de Física, Universidad Nacional Autónoma de México,  
Apartado Postal 20-364, Ciudad de México C.P. 01000, Mexico*

(Dated: April 25, 2023)

Magnons, the collective excitations of spin systems, have been proposed as a platform to induce conventional and unconventional superconductivity in magnetic solid-state devices. In this article, we study the induced interaction of spin-like collective excitations in an ultracold gas of hard-core bosons. We show that the induced interaction supports two-body states with energies, symmetries, and a number of bound states strongly dependent on the properties of the hard-core boson gas. The ability to control the nature of the two-body bound states motivates the study of superfluid phases, which we address within the BKT theory. We demonstrate how the superfluid parameters and critical temperatures can be tuned in our system. Our findings may pave the way for future theoretical and experimental studies with ultracold gases and solid-state systems.

## I. INTRODUCTION

Induced interactions play a fundamental role in many processes in physics, from phonon-induced Cooper pairing between electrons responsible for superconductivity [1, 2] to fundamental interactions in high-energy physics [3–5]. Engineering different mechanisms for tunable induced interactions has received notable attention in atomic and condensed matter physics. In the context of ultracold gases, the study of interactions mediated by the collective excitations of Bose gases has been extensively explored. Specifically, studies of phonon-like excitations of a weakly interacting Bose-Einstein condensate (BEC) have predicted intriguing few- and many-body phases, such as conventional superfluidity [6–11], topological superfluidity [12–16], bipolarons [17–24], and few-body states [25]. These studies have encouraged further investigation into the intrinsic nature of mediated interactions [26, 27] and the interaction between charged particles [28, 29]. Quantum microscopy delivered a powerful tool to explore phases of matter in optical lattices with site-by-site imaging [30], motivating the study of Bose lattice polarons [31], their mediated interactions [32] and strongly correlated physics with lattice Fermi polarons [33–41]. The development of new van der Waals heterostructures materials where a wide range of electronic and excitonic phases provides a scalable platform in which to realize complex phases of Bose-Fermi mixtures [42–48] previously studied with ultracold gases.

In magnetic materials coupled to a conductor [49], the interaction between the spins and the electrons in the conductor can induce an effective attraction between the electrons, leading to superconductivity [50–53]. Analogous to conventional superconductivity, which is mediated by phonons (the elementary excitations of the crystal), the collective excitations of the spins, termed magnons, lead to an attractive interaction between electrons. Magnon-mediated superconductivity has garnered

considerable attention, particularly for its potential to produce topological superconductivity phases [54, 55].

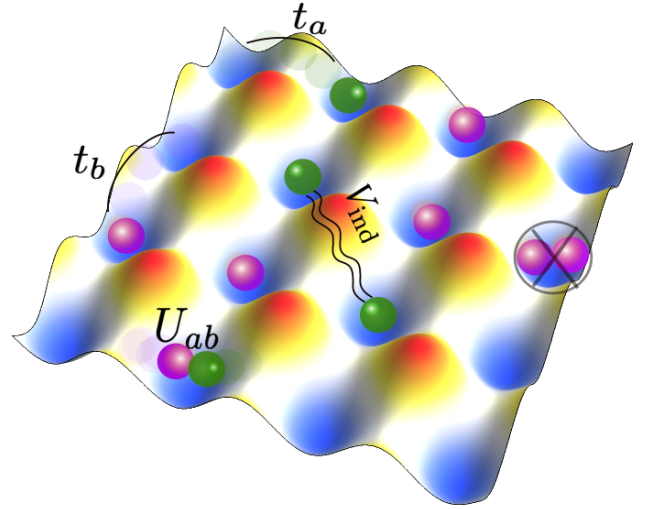


FIG. 1. A two-dimensional optical lattice confining a gas of hard-core bosons (purple balls) and a second species of atoms (greens balls). The collective excitations of the gas of hard-core bosons mediate an interaction between the minority atoms.

Ultracold gases are useful systems for emulating complex solid-state and condensed matter physics. In particular, when ultracold bosons are tightly confined to a two-dimensional lattice and subject to strong interactions, they exhibit collective excitations that resemble those of spin systems[56]. Recent experiments with moiré systems in van der Waals heterostructures have opened up new possibilities for studying collective modes analogous to those found in magnetic systems [57, 58]. Despite

this progress, however, the study of magnon-like excitations and their mediated interactions in ultracold gases remains largely unexplored.

In this article, we study the interaction induced by hard-core bosons and the emergence of two-body bound states, as well as mediated superfluidity. We show that the collective excitations of hard-core bosons, which resemble magnon-like excitations, mediate an interaction of a different character than the one induced by weakly interacting BECs. Here, we provide a comprehensive and self-contained study of the mediated interactions by hard-core bosons.

The remainder of the manuscript is organized in four main parts. In Sec. (II) we detail the model. Following Ref. [56] we discuss the elementary excitations of the gas of hard-core boson. Then, we derive the Fröhlich like Hamiltonian to describe the coupling between the collective excitations of the gas and a minority species coupled to the gas. This provides the necessary building blocks to derive the mediated interaction due to the exchange of spin-wave like excitations in the medium in Sec. (III). In Sec. (IV), we study the emergence of two-body bound states and demonstrate that the energy, number, and symmetries of the bound states can be varied over a wide range of parameters. Finally, in Sec. (V), we study mediated superfluidity, determining the superfluid parameter, the superfluid fraction, and the critical temperature within the Bardeen-Cooper-Schrieffer theory (BCS) and Berezinskii–Kosterlitz–Thouless (BKT) formalism. We conclude and provide an overlook of our findings in Sec. (VI).

Our studies may serve as a benchmark for future experiments and theories with ultracold atoms. Furthermore, our approach may be of interest to new quantum phases in van der Waals heterostructures, in particular, binary mixtures of electrons and excitons in flatbands, such as moiré lattices.

## II. MODEL

Our system of study consists of a gas of hard-core bosons (majority atoms) coupled to a few identical particles (minority atoms). The binary mixture is confined to a two-dimensional square optical lattice as illustrated in Fig. (1).

To make our manuscript self-contained, in this section we detail the system and present a short derivation of the collective excitations of the bosonic gas. We use this formalism to derive the coupling of the hard-core bosons to the second species of atoms in terms of the collective modes of the former. This section gives the theoretical background to address the study of mediated interaction by the exchange of magnon-like excitations. Readers already familiar with this first part can directly jump into Sec. (II B).

### A. Collective Excitations: Hard-Core Bosons

We start describing the collective excitations of the hard-core bosons. Our starting point is an ultracold gas of bosons confined to a two-dimensional square optical lattice of  $N_s$  sites. The Hamiltonian of the bosons is given by

$$\hat{H}_B = -t_b \sum_{\langle \mathbf{r}, \mathbf{r}' \rangle} (\hat{b}_{\mathbf{r}}^\dagger \hat{b}_{\mathbf{r}'} + \text{h.c.}) + \frac{U_{bb}}{2} \sum_{\mathbf{r}} \hat{b}_{\mathbf{r}}^\dagger \hat{b}_{\mathbf{r}}^\dagger \hat{b}_{\mathbf{r}} \hat{b}_{\mathbf{r}} - \mu_b \sum_{\mathbf{r}} \hat{b}_{\mathbf{r}}^\dagger \hat{b}_{\mathbf{r}}, \quad (1)$$

here  $\hat{b}_{\mathbf{r}}^\dagger$  creates a boson in site  $\mathbf{r}$ ,  $t_b$  is the nearest neighbour tunneling coefficient, the interaction between the bosons  $U_{bb}$  is assumed to be local, and  $\mu_b$  is the chemical potential.

We work in the regime where  $U_{bb} \gg t_b$  and assume that double occupation is strictly forbidden. That is, we impose the hard-core constraint for the majority bosons. Now, following Ref. [56] we introduce spin operators

$$\hat{b}_{\mathbf{r}}^\dagger \rightarrow \hat{S}_{\mathbf{r}}^\dagger, \text{ and } \hat{b}_{\mathbf{r}} \rightarrow \hat{S}_{\mathbf{r}}, \quad (2)$$

and map the Hamiltonian to a Heisenberg Hamiltonian of the form

$$\hat{H}_B = -t_b \sum_{\langle \mathbf{r}, \mathbf{r}' \rangle} (\hat{S}_{\mathbf{r}}^\dagger \hat{S}_{\mathbf{r}'} + \text{h.c.}) - \mu_b \sum_{\mathbf{r}} S_{\mathbf{r}}^z - \frac{\mu_b}{2} N_s, \quad (3)$$

which no longer explicitly depends on  $U_{bb}$ .

The mean-field solution is obtained assuming that all sites fill equally, and thus an ansatz for the ground-state is proposed as following

$$|\Psi\rangle = \prod_{\mathbf{r}} \left[ \sin\left(\frac{\theta}{2}\right) + \cos\left(\frac{\theta}{2}\right) \hat{S}_{\mathbf{r}}^\dagger \right] |0\rangle, \quad (4)$$

here the angle  $\theta$  is obtained by means of the variational principle  $\delta\langle\Psi|\hat{H}_B|\Psi\rangle/\delta\theta = 0$ . Upon minimizing the energy, one obtains for the variational parameter in terms of the chemical potential  $\theta = \mu_b/4t_b$ , which gives a filling factor of  $n_B = (\cos\theta + 1)/2$  and a condensate fraction  $n_0 = \sin^2\theta/4$ .

Now, we obtain the collective excitations. This is a two-step procedure where we first rotate our system to align the  $z$ -axis to the mean-field solution

$$\begin{bmatrix} \hat{S}_{\mathbf{r}}^x \\ \hat{S}_{\mathbf{r}}^y \\ \hat{S}_{\mathbf{r}}^z \end{bmatrix} = \begin{bmatrix} \cos\theta & 0 & \sin\theta \\ 0 & 1 & 0 \\ -\sin\theta & 0 & \cos\theta \end{bmatrix} \begin{bmatrix} \hat{L}_{\mathbf{r}}^x \\ \hat{L}_{\mathbf{r}}^y \\ \hat{L}_{\mathbf{r}}^z \end{bmatrix}. \quad (5)$$

Then we introduce the Holstein-Primakoff transformation by means of the operators  $\hat{d}_{\mathbf{r}}^\dagger$  and  $\hat{d}_{\mathbf{r}}$  assumed to be bosonic and given by

$$\begin{aligned} \hat{L}_{\mathbf{r}}^x &= \frac{1}{2}(\hat{d}_{\mathbf{r}}^\dagger + \hat{d}_{\mathbf{r}}), \\ \hat{L}_{\mathbf{r}}^y &= \frac{1}{2i}(\hat{d}_{\mathbf{r}}^\dagger - \hat{d}_{\mathbf{r}}), \\ \hat{L}_{\mathbf{r}}^z &= \frac{1}{2} - \hat{d}_{\mathbf{r}}^\dagger \hat{d}_{\mathbf{r}}. \end{aligned} \quad (6)$$

Grouping terms, we write the Hamiltonian as

$$\hat{H}_B \approx \sum_{\mathbf{k}} A_{\mathbf{k}} \left( \hat{d}_{\mathbf{k}}^\dagger \hat{d}_{\mathbf{k}} + \hat{d}_{-\mathbf{k}}^\dagger \hat{d}_{-\mathbf{k}} \right) + B_{\mathbf{k}} \left( \hat{d}_{\mathbf{k}}^\dagger \hat{d}_{-\mathbf{k}}^\dagger + \hat{d}_{-\mathbf{k}} \hat{d}_{\mathbf{k}} \right), \quad (7)$$

up to a constant energy shift [56]. Here, the  $A_{\mathbf{k}}$  and  $B_{\mathbf{k}}$  coefficients are given by,

$$A_{\mathbf{k}} = \frac{1}{2} \left[ \frac{\epsilon_{\mathbf{k}}}{2} (\cos^2 \theta + 1) + 4t_b \right], \quad (8)$$

$$B_{\mathbf{k}} = -\frac{1}{4} \sin^2 \theta \epsilon_{\mathbf{k}},$$

with  $\epsilon_{\mathbf{k}} = -2t_b (\cos(k_x a) + \cos(k_y a))$  where  $a$  is the lattice constant. Due to the quadratic form of the Hamiltonian, we perform a Bogoliubov transformation

$$\begin{aligned} \hat{d}_{\mathbf{k}} &= u_{\mathbf{k}} \hat{\gamma}_{\mathbf{k}} - v_{\mathbf{k}} \hat{\gamma}_{-\mathbf{k}}^\dagger \\ \hat{d}_{-\mathbf{k}}^\dagger &= u_{\mathbf{k}} \hat{\gamma}_{-\mathbf{k}}^\dagger - v_{\mathbf{k}} \hat{\gamma}_{\mathbf{k}} \end{aligned} \quad (9)$$

that takes the Hamiltonian to its diagonal form, and gives the collective excitations of the hard-core Bose gas

$$\hat{H}_B = \sum_{\mathbf{k}} \omega(\mathbf{k}) \hat{\gamma}_{\mathbf{k}}^\dagger \hat{\gamma}_{\mathbf{k}},$$

where the dispersion of the collective excitations is given by  $\omega(\mathbf{k}) = 2\sqrt{A_{\mathbf{k}}^2 - B_{\mathbf{k}}^2}$ . For small  $\mathbf{k}$ , the dispersion becomes linear

$$\omega(\mathbf{k}) \approx 2t_b a \sin \theta \sqrt{k_x^2 + k_y^2}. \quad (10)$$

This dispersion resembles the Bogoliubov dispersion of weakly interacting BECs; however, in this case, the interaction does not longer depend on the boson-boson interaction but solely on the tunneling coefficient and the angle  $\theta$ .

### B. Fröhlich Hamiltonian

A second species of atoms (minority) is placed in the two-dimensional optical lattice and couples to the hard-core bosons. The kinetic energy term of the second species is given by

$$\hat{H}_a = -t_a \sum_{\langle \mathbf{r}, \mathbf{r}' \rangle} \hat{a}_{\mathbf{r}}^\dagger \hat{a}_{\mathbf{r}'} + \text{h.c.}, \quad (11)$$

here  $t_a$  is the nearest-neighbour tunneling coefficient and  $\hat{a}_{\mathbf{r}}^\dagger$  creates an  $a$  atom in a given site  $\mathbf{r}$ . The coupling between the  $a$  and  $b$  atoms is short-ranged and local, described by the Hamiltonian

$$\hat{H}_{ab} = U_{ab} \sum_{\mathbf{r}} \hat{n}_b(\mathbf{r}) \hat{n}_a(\mathbf{r}), \quad (12)$$

where  $\hat{n}_{a,b}(\mathbf{r})$  are the number operator of the  $a/b$  atoms respectively. Here,  $U_{ab}$  can be tuned by means of a Feshbach resonance [59].

To make further progress, we are required to write the former interaction in terms of the collective excitations of the hard-core bosons. For such purpose, we write the Hamiltonian in terms of the  $d$  bosonic operators of the Holstein-Primakoff transformation

$$\begin{aligned} \hat{H}_{ab} &= \frac{U_{ab}}{2} (1 + \cos(\theta)) \sum_{\mathbf{r}} \hat{n}_a(\mathbf{r}) - \\ &\quad - \frac{U_{ab} \sin \theta}{2\sqrt{N_s}} \sum_{\mathbf{k}, \mathbf{q}} \left[ \hat{d}_{-\mathbf{q}}^\dagger + \hat{d}_{\mathbf{q}} \right] \hat{a}_{\mathbf{k}+\mathbf{q}}^\dagger \hat{a}_{\mathbf{k}}. \end{aligned} \quad (13)$$

The first term can be intuitively understood as the conventional mean-field correction  $U_{ab} n_B \sum_{\mathbf{r}} \hat{n}_a(\mathbf{r})$ , whereas the second line can be written in terms of the collective excitations  $\hat{\gamma}$  as follows

$$\hat{H}_F = \frac{1}{\sqrt{N_s}} V_F(\mathbf{q}) \left[ \hat{\gamma}_{-\mathbf{q}}^\dagger + \hat{\gamma}_{\mathbf{q}} \right] \hat{a}_{\mathbf{k}+\mathbf{q}}^\dagger \hat{a}_{\mathbf{k}}, \quad (14)$$

with the interaction between the  $a$  atoms and the collective excitations of the hard-core bosons

$$V_F(\mathbf{q}) = -\frac{1}{2} U_{ab} (u_{\mathbf{q}} - v_{\mathbf{q}}) \sin \theta. \quad (15)$$

For the Fröhlich-like Hamiltonian, we only retain as usual linear terms in the collective excitations.

### III. MEDIATED INTERACTION

We have now collected the elements to derive the interactions between the  $a$  atoms mediated by the collective excitations of the hard-core boson gas. Our starting point is the Hamiltonian written in terms of the  $d$  operators, after having performed the Holstein-Primakoff transformation.

We derive the mediated interaction following a field theoretical approach where we trace over the collective modes of the hard-core bosons [60]. We introduce the action

$$\begin{aligned} S(\psi_a^*, \psi_a, \phi_d^*, \phi_d) &= S_d(\phi_d^*, \phi_d) + S_a(\psi_a^*, \psi_a) \\ &\quad + S_{ab}(\psi_a^*, \psi_a, \phi_d^*, \phi_d). \end{aligned} \quad (16)$$

here, the action  $S_d(\phi_d^*, \phi_d)$  depends on the bosonic fields  $\phi_d$  and is given by

$$S_d(\phi_d^*, \phi_d) = \sum_k \Phi_d^*(k) \cdot [-\mathcal{G}_d^{-1}(k)] \cdot \Phi_d(k), \quad (17)$$

with  $\Phi_d^*(k) = [\phi_d^*(k), \phi_d(-k)]$ . The Green's function of the  $d$ -bosons is given by

$$\mathcal{G}_d^{-1}(k) = \begin{bmatrix} -i\nu_n + A_{\mathbf{k}} & B_{\mathbf{k}} \\ B_{\mathbf{k}} & i\nu_n + A_{\mathbf{k}} \end{bmatrix} \quad (18)$$

where  $k = (\mathbf{k}, i\nu_n)$  with  $\nu_n$  a bosonic Matsubara frequency.

The action accounting for the coupling between the  $a$  atoms and the bosons is given by

$$S_{ab}(\psi_a^*, \psi_a, \phi_d^*, \phi_d) = \frac{1}{\sqrt{N_s}} \sum_q \Phi_d^*(q) \cdot J_a(q) + J_a^*(q) \cdot \Phi_d(q), \quad (19)$$

with  $J_a^*(q) = \frac{U_{ab}}{2} \sum_k \psi_a^*(k) \psi_a(k+q)(1,1)$ . Finally, the action of the  $a$  atoms is

$$S_a(\psi^*, \psi) = - \sum_q \psi_a(q)(i\nu_n - \epsilon_{\mathbf{q}}) \psi_a(q).$$

From the grand partition function  $Z = \int d\phi_d d\psi_b d\phi_d^* d\psi_b^* \exp[-S(\psi_a^*, \psi_a, \phi_d^*, \phi_d)]$ , we perform the Gaussian integral over the  $d$ -fields which traces out these degrees of freedom. The effective action depending only on the  $a$ -field is  $S_{\text{eff}}(\psi_a^*, \psi_a) = S_a(\psi_a^*, \psi_a) + S_{\text{ind}}(\psi_a^*, \psi_a)$ , where  $S_{\text{ind}}(\psi_a^*, \psi_a)$ , arises from the trace and is given by

$$\begin{aligned} S_{\text{ind}}(\psi^*, \psi) &= J_a^*(q) \cdot \mathcal{G}_d(q) \cdot J_a(q) = \\ &= \frac{U_{ab}^2}{2N_s} \sum_q \rho_a(q) \frac{A_{\mathbf{q}} - B_{\mathbf{q}}}{i\nu_n^2 - (A_{\mathbf{q}}^2 - B_{\mathbf{q}}^2)} \sin^2 \theta \rho_a(q), \end{aligned} \quad (20)$$

here  $\rho_a(q) = \sum_k \psi_a^*(k) \psi_a(k+q)$ . This term is quartic in the  $a$  fields and corresponds to a mediated interaction due to the exchange of a collective mode of the hard-core Bose gas.

To understand the character of the mediated interaction let us focus on the static interaction, given by

$$V_{\text{ind}}(\mathbf{q}) = - \frac{U_{ab}^2}{4t_b + \cos^2 \theta \epsilon_{\mathbf{q}}} \sin^2 \theta, \quad (21)$$

as expected, the induced interaction is quadratic in  $U_{ab}$  and linear in the condensate density  $n_0 \propto \sin^2 \theta$ . Interestingly, the zero-momentum limit of the induced interaction is independent of  $\theta$ , that is, it does not depend on the filling factor of the bosons,

$$\lim_{\mathbf{q} \rightarrow 0} V_{\text{ind}}(\mathbf{q}) \propto - \frac{U_{ab}^2}{t_b}. \quad (22)$$

This induced interaction exhibits similarities and striking differences with the interaction mediated by weakly interacting BECs [61–63]. Firstly, as in the case of phonon-mediated interaction, the zero-energy momentum of the induced interaction is independent of the density of the medium. However, for a weakly interacting BEC ( $U_{bb} \ll t_b$ ), the limit is given by  $\lim_{\mathbf{q} \rightarrow 0} V_{\text{ind}}(\mathbf{q}) = -\frac{U_{ab}^2}{U_{bb}}$  and is independent of  $t_b$ . For hard-core bosons, the zero-energy momentum limit is, of course, independent of  $U_{bb}$  and scales inversely proportional to  $t_b$ . Furthermore, we also note that the potential in Eq. (21) is symmetric around  $\theta = \pi/2$ , that is, invariant under the exchange of  $n_B \rightarrow (1 - n_B)$ , reflecting the particle-hole symmetry of the underlying Hamiltonian governing the bosonic bath.

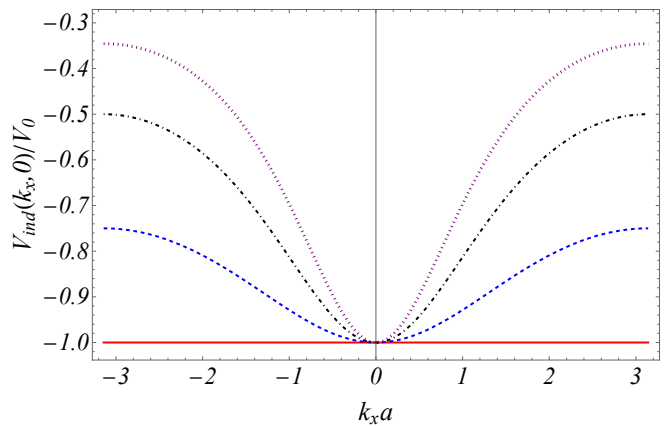


FIG. 2. Mediated interaction as a function of  $k_x a$  for fixed  $k_y a = 0$ . The solid red curve corresponds to half-filling ( $\theta = \pi/2$ ), the blue dashed lines gives the induced interaction for  $\theta = \pi/3$ , whereas  $\theta = \pi/4$  is shown by the dot-dashed black line. Finally, the purple line illustrates the mediated interaction for  $\theta = \pi/5$ .

To gain intuition about the form of the induced interaction, we show in Fig. (2) a cross-section of  $V_{\text{ind}}(\mathbf{q})$  for  $k_y = 0$  and as a function of  $k_x$  for several values of angle  $\theta$ . The solid red line corresponds to half-filling ( $\theta = \pi/2$ ). In this case, the induced interaction becomes independent of  $\mathbf{k}$  and gives a short-ranged purely on-site interaction. With varying angle, we show that the induced interaction acquires more structure, as shown for  $\theta = \pi/3$  (dashed blue),  $\theta = \pi/4$  (dot dashed black), and  $\theta = \pi/5$  (purple dots). For clarity, we show in units of  $V_0 = U_{ab}^2/4t_b$ .

Figure (2) illustrates the strong dependence of the induced interaction on the filling factor of the hard-core boson gas. In particular, the character of the mediated interaction can be controlled via the angle  $\theta$ . For  $\theta = \pi/2$  the induced interaction is short-ranged and local (contact interaction) while away from half-filling the mediated interaction acquires spatial structure and becomes a finite range-potential where atoms scatter beyond the on-site interaction term. That is, the momentum dependence of the induced interaction in momentum space implies that the interaction in real space is no longer solely on-site interaction.

#### IV. BOUND STATES

Motivated by the possibility of tuning the intrinsic character of the mediated interaction, we turn our attention to the study of the two-body bound states appearing as a consequence of the induced interaction. In this case, we study the Schrödinger equation for a pair of  $a$ -atoms interacting via the static mediated interaction, that is,

$$E\psi(\mathbf{k}) = 2\epsilon_{\mathbf{k}}\psi(\mathbf{k}) + \frac{1}{N_s} \sum_{\mathbf{q}} V_{\text{ind}}(\mathbf{k} - \mathbf{q})\psi(\mathbf{q}) \quad (23)$$

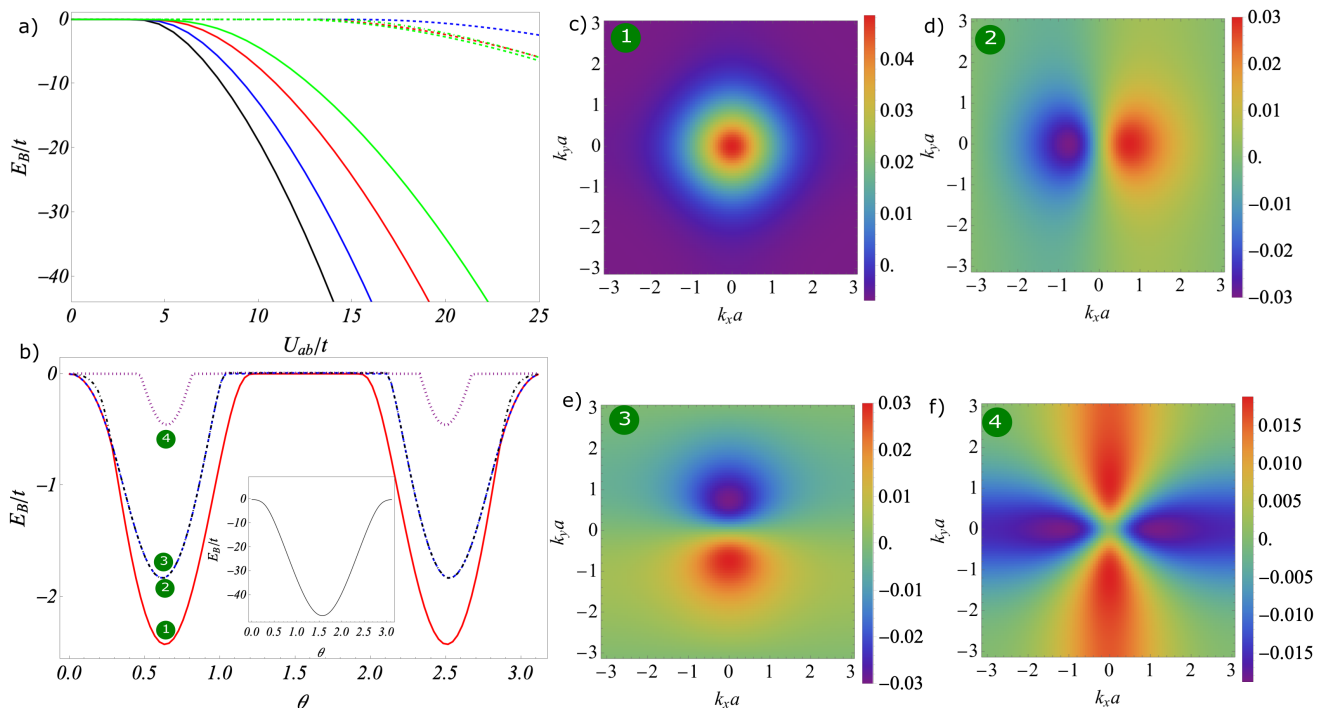


FIG. 3. Two-body bound states. (a) Binding energies as a function of  $U_{ab}/t$  for  $\theta = \pi/2$  (black),  $\theta = \pi/3$  (blue),  $\theta = \pi/4$  (red) and  $\theta = \pi/5$  (green). The solid lines give the lowest bound state for each angle whereas the dashed lines correspond to excited (bound) states. Panel (b) shows the binding energies as a function of  $\theta$  for  $U_{ab}/t = 20$ . The red line gives the first excited state. Above the first excited state, we obtain two degenerate states (blue and black on top of each other) and a fourth excited bound state marked by the purple line. The inset gives the lowest bound state energy for  $U_{ab}/t = 10$ . Panels (c) to (f) show the real part of the wave function for the points (1)-(4) marked by the green circles in panel (b) giving different symmetries: from  $s$ - to  $p$ - and  $d$ - wave.

where  $\psi(\mathbf{k})$  is the wave function of the relative coordinate. We have written the Schrödinger equation in its conventional form in momentum space.

Figure (3) summarises the main features of the two-body bound states as a function of the tuneable parameters of the system.

First, Fig. (3)(a) shows the binding energy  $E_b$  defined as  $E = E_b - 2\epsilon_{\mathbf{k}=0}$  as a function of  $U_{ab}/t$  for several filling fractions. Here, we have taken  $t_a = t_b = t$ . For  $\theta = \pi/2$  (solid black), we only find one bound state regardless of how large  $U_{ab}/t$  is tuned. This is a consequence of the nature of the induced interaction at half-filling: the contact interaction supports a single bound state. On the other hand, for  $\theta = \pi/3$  (blue),  $\theta = \pi/4$  (red), and  $\theta = \pi/5$  (green), we also find a lower-lying bound state with an energy slightly above the bound state for  $\theta = \pi/2$ . However, away from half-filling, we find that the induced interaction supports multiple bound states. Therefore, giving spatial structure to the mediated interactions yields a rich family of two-body bound states absent at  $\theta = \pi/2$ .

The role of the filling factor in the emergence of many two-body bound states is clarified in Fig. (3)(b). Here, we plot the second to fifth lowest bound states as a function of  $\theta$  for  $U_{ab}/t = 20$ . First, as discussed previously, the emergence of a second bound state is very suppressed close to half-filling due to the character of the induced

potential. On the other hand, we observe several bound states at different angles, whose energy becomes maximal close to  $\pi/5$ . In this case, we find a non-degenerate second lowest bound state (solid red line), two degenerate states marked by the blue and black dashed lines (which overlap), and an additional bound state with a smaller binding energy shown in purple. The energy of the lowest bound state is illustrated in Fig. (3)(b, inset) and shows that the lowest bound state energy lies far below the energy of the highest bound states.

The nature of these bound states is unveiled by the wave-function of the states, which reveals the symmetries of the states. In our case, we find that the lowest bound state is always spherically symmetric (not shown). However, the excited states do acquire structure. In Fig. (3)(c)-(f), we show the real part of the wave-function over the first Brillouin zone for the bound states marked by the green circles in Fig. (3)(b), around  $\theta = \pi/5$ , where the excited bound state peaks. The first excited state (second lowest bound state) is also spherically symmetric. The second and third excited states are degenerate in energy and exhibit a  $p$ -wave symmetry. Finally, the highest excited bound state possesses a  $d$ -wave symmetry.

The symmetry of the wavefunction is intrinsically linked to the statistics of the second species of atoms. For

bosonic atoms or fermions in a different internal state, the allowed symmetries are the  $s$ - and  $d$ -wave wavefunctions. On the other hand, for fermions (spin-polarized), the wavefunction is required to be anti-symmetric in  $\mathbf{k}$ , that is,  $\psi(\mathbf{k}) = -\psi(-\mathbf{k})$ , the permitted states are therefore the  $p$ - wave states in Fig. (3) (d) and (e).

Our analysis demonstrates that the energy, number, and symmetry of two-body bound states induced by an indirect interaction mediated by the exchange of spin-like excitations can be tuned over a wide range of parameters by means of the filling factor and the strength of the indirect coupling. We note that, although multiple bound states only appear away from half-filling, the most robust two-body state appears at  $\theta = \pi/2$ .

In homogeneous and lattice systems, weakly interacting Bose-Einstein condensates have proven to provide an effective mechanism to induce superfluid phases including  $s$ - wave and topological superfluidity [6–16]. Spin-wave mediated interactions also provide an attractive interaction, which we have demonstrated supports several two-body bound states. Now, in the following section we explore the presence of superfluidity mediated by the exchange of collective excitations.

## V. MEDIATED SUPERFLUIDITY

Having understood the consequence of the mediated interactions in the emergence of two-body bound states, we now explore the possibility of inducing superfluidity. Specifically, we consider a binary and spin-balanced mixture of fermions embedded in a gas of hard-core bosons. The effective Hamiltonian of the fermions is given by

$$\hat{H}_{\text{eff}} = -t \sum_{\sigma} \sum_{\langle \mathbf{r}, \mathbf{r}' \rangle} (\hat{a}_{\mathbf{r}\sigma}^{\dagger} \hat{a}_{\mathbf{r}'\sigma} + \text{h.c.}) - \mu \sum_{\mathbf{r}} \hat{a}_{\mathbf{r}\sigma}^{\dagger} \hat{a}_{\mathbf{r}\sigma} + \sum_{\mathbf{r}, \mathbf{r}'} V_{\text{ind}}(\mathbf{r} - \mathbf{r}') \hat{a}_{\mathbf{r}\uparrow}^{\dagger} \hat{a}_{\mathbf{r}'\downarrow}^{\dagger} \hat{a}_{\mathbf{r}'\downarrow} \hat{a}_{\mathbf{r}\uparrow}. \quad (24)$$

here, the operators  $\hat{a}_{\mathbf{r}\sigma}^{\dagger}$  create a fermion with spin  $\sigma = \uparrow / \downarrow$  in a given site  $\mathbf{r}$ . We consider a chemical potential  $\mu$  independent of the spin  $\sigma$ . The fermions only interact via the interaction  $V_{\text{ind}}(\mathbf{r} - \mathbf{r}')$  discussed previously.

For this purpose, we write the Hamiltonian in the standard BCS form

$$\hat{H}_{\text{BCS}} = \frac{1}{2} \sum_{\mathbf{k}} [\hat{a}_{\mathbf{k}\uparrow}^{\dagger} \hat{a}_{-\mathbf{k}\downarrow}] \cdot \begin{bmatrix} \xi_{\mathbf{k}} & \Delta_{\mathbf{k}} \\ \Delta_{\mathbf{k}}^* & -\xi_{\mathbf{k}} \end{bmatrix} \cdot \begin{bmatrix} \hat{a}_{\mathbf{k}\uparrow} \\ \hat{a}_{-\mathbf{k}\downarrow}^{\dagger} \end{bmatrix}, \quad (25)$$

where the superfluid gap and number equations

$$\Delta_{\mathbf{k}} = -\frac{1}{2N_s} \sum_{\mathbf{q}} V_{\text{ind}}(\mathbf{k} - \mathbf{q}) \frac{\Delta_{\mathbf{q}}}{E_{\mathbf{q}}} \tanh\left(\frac{E_{\mathbf{q}}}{2T}\right), \quad (26)$$

$$n = \frac{1}{2} \left( 1 - \frac{1}{N_s} \sum_{\mathbf{q}} \frac{\xi_{\mathbf{q}}}{E_{\mathbf{q}}} \tanh\left(\frac{E_{\mathbf{q}}}{2k_B T}\right) \right), \quad (27)$$

respectively. Here, the dispersion of the BCS superfluid is given by  $E_{\mathbf{k}} = \sqrt{\xi_{\mathbf{k}}^2 + \Delta_{\mathbf{k}}^2}$ . We include the Hartree-Fock contribution  $\xi_{\mathbf{k}} = \epsilon_{\mathbf{k}} + \Sigma_{\mathbf{k}} - \mu$  with the self-energy term given by

$$\Sigma_{\mathbf{k}} = \sum_{\mathbf{q}} \frac{[V_{\text{ind}}(\mathbf{0}) - V_{\text{ind}}(\mathbf{k} - \mathbf{q})]}{2N_s} \left[ 1 - \frac{\xi_{\mathbf{q}}}{E_{\mathbf{q}}} \tanh\left(\frac{E_{\mathbf{q}}}{2k_B T}\right) \right]. \quad (28)$$

Here  $k_B$  is the Boltzmann constant and  $T$  the temperature.

In addition, we introduce the superfluid stiffness parameter

$$J_{i,j} = \frac{1}{4N_s a^2} \sum_{\mathbf{k}} \left( n(\mathbf{k}) \frac{\partial^2 \epsilon_{\mathbf{k}}}{\partial k_i \partial k_j} - Y(\mathbf{k}) \frac{\partial \epsilon_{\mathbf{k}}}{\partial k_i} \frac{\partial \epsilon_{\mathbf{k}}}{\partial k_j} \right), \quad (29)$$

where  $n(\mathbf{k}) = |u_{\mathbf{k}}|^2 f(E_{\mathbf{k}}) + |v_{\mathbf{k}}|^2 (1 - f(E_{\mathbf{k}}))$ , where  $u_{\mathbf{k}}, v_{\mathbf{k}}$  are the standard BCS Bogoliubov factors  $u_{\mathbf{k}}^2 = (1 + \xi_{\mathbf{k}}/E_{\mathbf{k}})/2$  and  $u_{\mathbf{k}}^2 + v_{\mathbf{k}}^2 = 1$  [14]. And the Yoshida function  $Y(\mathbf{k}) = 1/4k_B T \text{sech}(E_{\mathbf{k}}/2T)$ .

*Superfluidity.*- We are now in position to study the emergence of superfluid phases. From our previous analysis of the two-body bound states, we expect the  $s$ - wave to be the dominant contribution to the superfluid parameter. We find numerically that, indeed, for the parameters explored the gap  $\Delta_{\mathbf{k}}$  is essentially independent of  $\mathbf{k}$ .

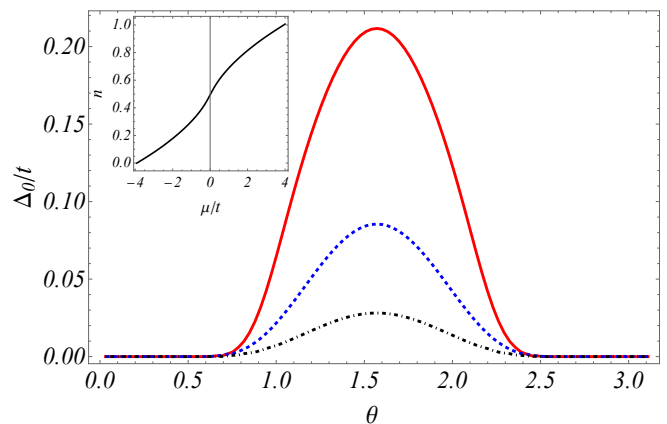


FIG. 4. Superfluid gap as a function of  $\theta$  for  $\mu/t = -2$  (dotted black line) and  $\mu/t = -1$  (dashed blue line) and  $\mu/t = 0$  (solid red line). (Inset) Fermions per site as a function of the chemical potential  $\mu/t$  for  $\theta = \pi/2$ .

We now explore the emergence of superfluid phases as a function of the angle  $\theta$  and at zero temperature. In Fig. (4), we show the superfluid parameter  $\Delta_0$  for several values of the fermion chemical potential  $\mu$ , with  $U_{ab}/t$  fixed at 2.5. We observe the same qualitative behavior of the gap parameter as in the lowest two-body bound state studied previously: the superfluid parameter is maximal at  $\pi/2$ , and decreases away from half-filling of bosons. Finally, at large angles, the superfluid gap vanishes. We show results for  $\mu/t = 0$  (solid red line),

$\mu/t = -1$  (dashed black line), and  $\mu/t = -2$  (dot dashed black line). As an inset, we show the fermion density as a function of the chemical potential  $\mu$ . We find that the number of fermions  $n$ , given in terms of  $\mu$ , is largely independent of  $\theta$ .

The superfluid parameter primarily arises from  $s$ -wave scattering and peaks around  $\theta = \pi/2$ . The dependence on  $\theta$  can also be intuitively understood from the condensate fraction of bosons, which scales with the filling factor as  $n_0 = n_B(1 - n_B) = \sin^2\theta/4$ . That is, the condensate fraction becomes maximal at  $\theta = \pi/2$  and induces an attractive interaction more efficiently around this angle. Away from half-filling of bosons, the induced interaction becomes suppressed and unable to effectively induce fermion  $s$ -wave pairing.

Now, we will explore the stiffness parameter as a function of temperature. In this case, we keep  $U_{ab}/t = 2.5$  and the bosonic filling factor  $\theta = \pi/2$  fixed. We show the same values of the chemical potential of the fermions as before, using the same color codes:  $\mu/t = 0$  (solid red line),  $\mu/t = -1$  (dashed black line), and  $\mu/t = -2$  (dot-dashed black line).

Consistent with the results of Fig. (4), we find in Fig. (5) that the stiffness parameter is larger for the same set of parameters for which the superfluid gap is larger. According to the BCS theory, we find that the stiffness and superfluid gap parameters are continuous functions of temperature. The stiffness parameter vanishes above a critical temperature  $T_{\text{BCS}}$ , indicated by the square marks in Fig. (5).

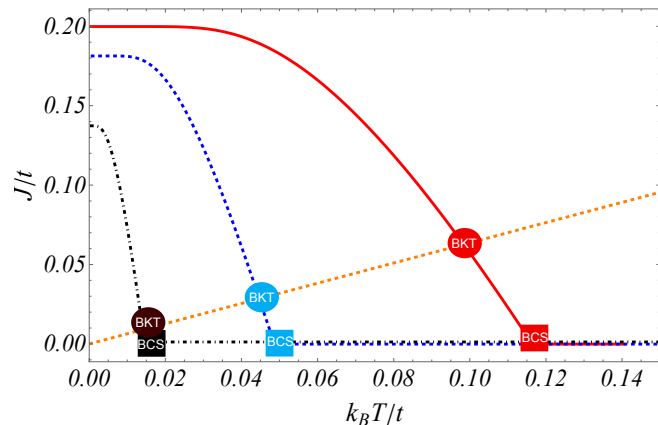


FIG. 5. The stiffness parameter is shown as a function of temperature for three different values of the chemical potential of the fermions:  $\mu/t = -2$  (dot-dashed black line),  $\mu/t = -1$  (dashed blue line), and  $\mu/t = 0$  (solid red line). The critical BCS temperature is marked by filled squares in the figure, as the stiffness parameter vanishes above this temperature. Additionally, the filled circles indicate the critical BKT temperature given by Eq. (30). These correspond to the intersection between the stiffness parameter curves and the dashed orange line in the figure. Notably, we observe that the stiffness parameter is larger for parameters with larger superfluid gap, consistent with the behavior observed in Fig. (4).

*Berezinskii–Kosterlitz–Thouless Superfluidity.*— It is well-established that two-dimensional systems cannot exhibit conventional long-range order. Instead, the transition is governed by the Berezinskii–Kosterlitz–Thouless theory (BKT). We obtain the BKT transition temperature from the expression: [12, 64–68]

$$J(T_{\text{BKT}}) = \frac{2}{\pi} k_B T_{\text{BKT}}. \quad (30)$$

Graphically, the BKT critical temperature is obtained from the crossing point of the orange dashed line, which represents  $\frac{2}{\pi} k_B T$ , and the stiffness parameter in Fig. (5). From Fig. (5), we observe that if the BCS critical temperature is small, then the BKT and BCS critical temperatures tend to agree (dot-dashed black line). However, as the BCS critical temperature increases, we observe significant deviations from the BKT theory prediction.

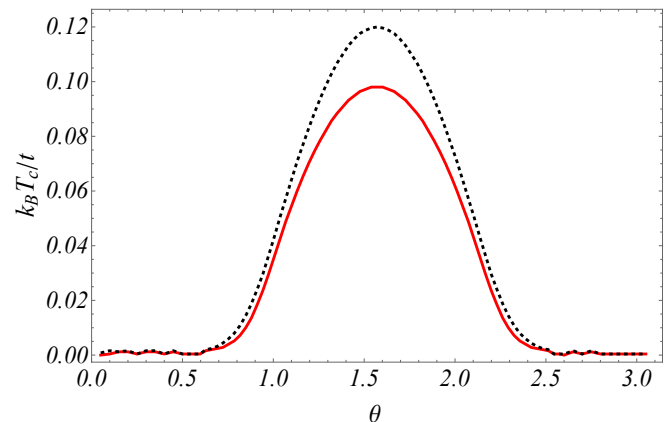


FIG. 6. Critical transition within the BKT formalism (solid line) and the BCS theory (dashed line) as a function of  $\theta$  for  $\mu/t = 0$  (red).

To quantitatively analyze the discrepancies between the BKT and BCS critical temperature, we plot in Fig. (6) the critical temperatures obtained from the BCS theory (dashed black) and the BKT formalism (solid red), as a function of  $\theta$  for  $\mu/t = 0$  and  $U_{ab}/t = 2.5$ . We observe that away from half-filling, the BCS critical temperature agrees remarkably well with the BKT prediction. However, as the BCS critical temperature increases closer to  $\theta = \pi/2$ , the BCS theory deviates from the BKT theory.

Figure (6) illustrates that the BKT critical temperature follows the same qualitative behavior as the superfluid gap in Fig. (5). That is, the critical temperature is higher around half-filling of bosons than at small/large angles where the condensate fraction vanishes and the induced interaction becomes very inefficient. The maximal critical temperature is around  $k_B T_{\text{BKT}}/t \approx 0.12$ , which gives a typical temperature of several  $nK$ , which is of the order of magnitude of the state-of-the-art experiments with ultracold atoms.

Finally, we study the critical temperature as a function

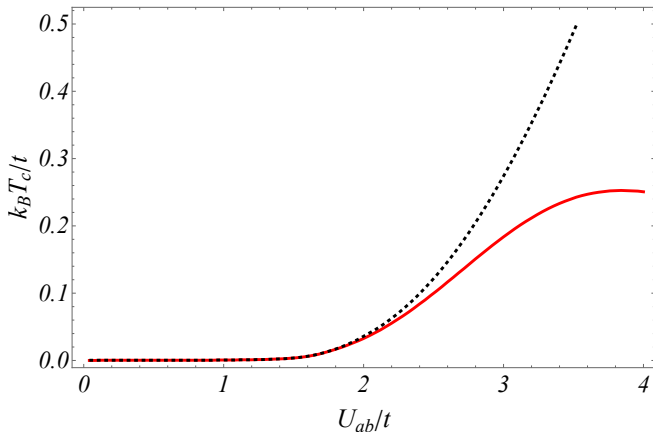


FIG. 7. Critical temperature as a function of  $U_{ab}$  in black the BCS critical temperature while the red line gives the BKT critical temperature.

of the coupling strength  $U_{ab}$  for fixed  $\theta = \pi/2$ , and chemical potential  $\mu/t = 0$ . We plot in Fig. (7) the BKT (solid red line) and the BCS (dashed black line) critical temperature. We find that as long as  $U_{ab}/t$  is kept small, both the BKT and BCS critical temperatures agree very well. With increasing  $U_{ab}/t$ , the critical temperature starts to deviate, while the BCS theory completely overestimates the transition temperature and increases without bound as  $U_{ab}$  is increased, the BKT temperature saturates.

Conventional  $s$ -wave superfluidity can emerge as a consequence of magnon-like interactions which becomes maximal when the induced interaction is purely  $s$ -wave, that is, a mediated contact interaction. For weak boson-fermion interaction the BCS theory suffices to describe the critical temperature of the transition to superfluid. However, with increasing boson-fermion coupling we obtain visible corrections to the BCS predictions via the BKT formalism.

## VI. DISCUSSION AND CONCLUSIONS

Induced interactions play a crucial role in mediating collective phenomena in many quantum many-body systems. Magnon-induced interactions have emerged as a promising mechanism for generating exotic phases of matter. In this article, we demonstrate the analogue of

spin wave excitations in an ultracold gas of hard-core bosons and show that magnon-like excitations are suitable for generating two-body bound states and mediating conventional superfluidity.

From a two-body perspective, we show that the filling factor of the bath can be used to control and manipulate the energy, number, and symmetry of the emerging two-body bound states. Although the bound states become more stable at half-filling, at this filling, only a single bound state emerges, and its symmetry is constrained to  $s$ -wave. Away from half-filling, we illustrate additional bound states with  $s$ ,  $p$ , and  $d$ -wave symmetries.

Finally, we study mediated superfluidity within the BCS and BKT formalisms. We determine the gap parameter, superfluid stiffness, and BKT critical temperature and demonstrate that superfluidity becomes maximal close to the half-filling of bosons.

Our approach makes some approximations that we now discuss. First, we assume that the ground state of the hard-core bosons remains unaltered in the presence of fermions. We expect this approximation to be valid as long as the density of fermions remains smaller than the density of bosons. Second, we assume that the induced interaction is static. This is accurate as long as the typical exchanged energies between the fermions remain smaller than  $t_b$ , thus  $\Delta/t_b \ll 1$ .

Our study raises new questions related to the study of mediated interactions in van der Waals heterostructures, particularly moiré setups where Hubbard physics naturally appears, and the analysis of similar phases with Bose-Fermi mixtures of excitons and electrons [58, 69–72]. Another question relates to the study of mediated interactions when the underlying bath is in a strongly correlated phase such as a supersolid [58] and studies beyond the contact interaction for the boson-fermion direct interaction [73, 74].

## VII. ACKNOWLEDGMENTS

A. C. G. thanks R. Paredes for the reading of the manuscript. M. S. G acknowledges to Consejo Nacional de Ciencia y Tecnología (CONACYT) for the scholarship provided. A.C.G. acknowledges financial support from UNAM DGAPA PAPIIT Grants No. IA101923 and UNAM DGAPA PAPIIME Grants No. PE101223.

- 
- [1] Leon N. Cooper, “Bound electron pairs in a degenerate fermi gas,” *Phys. Rev.* **104**, 1189–1190 (1956).  
 [2] J. Bardeen, L. N. Cooper, and J. R. Schrieffer, “Theory of superconductivity,” *Phys. Rev.* **108**, 1175–1204 (1957).  
 [3] Hideki Yukawa, “On the interaction of elementary particles. i,” *Proceedings of the Physico-Mathematical Society of Japan. 3rd Series* **17**, 48–57 (1935).

- [4] Hideki Yukawa and Shoichi Sakata, “On the interaction of elementary particles ii,” *Proceedings of the Physico-Mathematical Society of Japan. 3rd Series* **19**, 1084–1093 (1937).  
 [5] Melvin A Ruderman and Charles Kittel, “Indirect exchange coupling of nuclear magnetic moments by conduction electrons,” *Physical Review* **96**, 99 (1954).

- [6] D.-W. Wang, M. D. Lukin, and E. Demler, “Engineering superfluidity in bose-fermi mixtures of ultracold atoms,” *Phys. Rev. A* **72**, 051604 (2005).
- [7] Daw-Wei Wang, “Strong-coupling theory for the superfluidity of bose-fermi mixtures,” *Physical review letters* **96**, 140404 (2006).
- [8] Michael Pasek and Giuliano Orso, “Induced pairing of fermionic impurities in a one-dimensional strongly correlated bose gas,” *Physical Review B* **100**, 245419 (2019).
- [9] Mônica Andrioli Caracanhas, F Schreck, and C Morais Smith, “Fermi–bose mixture in mixed dimensions,” *New Journal of Physics* **19**, 115011 (2017).
- [10] Ziyue Wang and Lianyi He, “Superfluid density reduction and spin-imbalanced pairing in a fermionic superfluid due to dynamical boson exchange,” *Physical Review A* **99**, 033620 (2019).
- [11] OI Matsyshyn, AI Yakimenko, EV Gorbar, SI Vilchinskii, and VV Cheianov, “p-wave superfluidity in mixtures of ultracold fermi and spinor bose gases,” *Physical Review A* **98**, 043620 (2018).
- [12] Zhigang Wu and G. M. Bruun, “Topological superfluid in a fermi-bose mixture with a high critical temperature,” *Phys. Rev. Lett.* **117**, 245302 (2016).
- [13] Jami J. Kinnunen, Zhigang Wu, and Georg M. Bruun, “Induced  $p$ -wave pairing in bose-fermi mixtures,” *Phys. Rev. Lett.* **121**, 253402 (2018).
- [14] Jonatan Melkær Midtgaard, Zhigang Wu, and G. M. Bruun, “Time-reversal-invariant topological superfluids in bose-fermi mixtures,” *Phys. Rev. A* **96**, 033605 (2017).
- [15] Yongzheng Wu, Zheng Yan, Zhi Lin, Jie Lou, and Yan Chen, “Effective p-wave fermi-fermi interaction induced by bosonic superfluids,” *Scientific Reports* **10**, 10822 (2020).
- [16] Junhua Zhang, Sumanta Tewari, and VW Scarola, “Stabilizing topological superfluidity of lattice fermions,” *Physical Review A* **104**, 033322 (2021).
- [17] A. S. Dekharghani, A. G. Volosniev, and N. T. Zinner, “Coalescence of two impurities in a trapped one-dimensional bose gas,” *Phys. Rev. Lett.* **121**, 080405 (2018).
- [18] Arturo Camacho-Guardian, LA Peña Ardila, Thomas Pohl, and Georg M Bruun, “Bipolarons in a bose-einstein condensate,” *Physical review letters* **121**, 013401 (2018).
- [19] Aleksandra Petković and Zoran Ristivojevic, “Mediated interaction between polarons in a one-dimensional bose gas,” *Physical Review A* **105**, L021303 (2022).
- [20] Christos Charalambous, Miguel A Garcia-March, Aniello Lampo, Mohammad Mehboud, and Maciej Lewenstein, “Two distinguishable impurities in bec: squeezing and entanglement of two bose polarons,” *SciPost Physics* **6**, 010 (2019).
- [21] LA Peña Ardila, GE Astrakharchik, and Stefano Giorgini, “Strong coupling bose polarons in a two-dimensional gas,” *Physical Review Research* **2**, 023405 (2020).
- [22] Friethjof Theel, Simeon I Mistakidis, and Peter Schmelcher, “Crossover from attractive to repulsive induced interactions and bound states of two distinguishable bose polarons,” *arXiv preprint arXiv:2303.04699* (2023).
- [23] Jonas Jager and Ryan Barnett, “The effect of boson–boson interaction on the bipolaron formation,” *New Journal of Physics* **24**, 103032 (2022).
- [24] Martin Will, Gregory E Astrakharchik, and Michael Fleischhauer, “Polaron interactions and bipolarons in one-dimensional bose gases in the strong coupling regime,” *Physical review letters* **127**, 103401 (2021).
- [25] Pascal Naidon, “Two impurities in a bose–einstein condensate: From yukawa to efimov attracted polarons,” *Journal of the Physical Society of Japan* **87**, 043002 (2018), <https://doi.org/10.7566/JPSJ.87.043002>.
- [26] Keisuke Fujii, Masaru Hongo, and Tilman Enss, “Universal van der waals force between heavy polarons in superfluids,” *Physical Review Letters* **129**, 233401 (2022).
- [27] Benjamin Reichert, Aleksandra Petković, and Zoran Ristivojevic, “Field-theoretical approach to the casimir-like interaction in a one-dimensional bose gas,” *Physical Review B* **99**, 205414 (2019).
- [28] Shanshan Ding, Michael Drewsen, Jan J Arlt, and GM Bruun, “Mediated interaction between ions in quantum degenerate gases,” *Physical Review Letters* **129**, 153401 (2022).
- [29] Grigory E Astrakharchik, Luis A Peña Ardila, Krzysztof Jachymski, and Antonio Negretti, “Many-body bound states and induced interactions of charged impurities in a bosonic bath,” *Nature Communications* **14**, 1647 (2023).
- [30] Waseem S. Bakr, Jonathon I. Gillen, Amy Peng, Simon Fölling, and Markus Greiner, “A quantum gas microscope for detecting single atoms in a hubbard-regime optical lattice,” *Nature* **462**, 74–77 (2009).
- [31] V. E. Colussi, F. Caleffi, C. Menotti, and A. Recati, “Lattice polarons across the superfluid to mott insulator transition,” (2022).
- [32] Shanshan Ding, G. A. Domínguez-Castro, Alekski Julku, Arturo Camacho-Guardian, and Georg M. Bruun, “Polarons and bipolarons in a two-dimensional square lattice,” *arXiv e-prints*, arXiv:2212.00890 (2022), arXiv:2212.00890 [cond-mat.quant-gas].
- [33] K. K. Nielsen, M. A. Bastarrachea-Magnani, T. Pohl, and G. M. Bruun, “Spatial structure of magnetic polarons in strongly interacting antiferromagnets,” *Phys. Rev. B* **104**, 155136 (2021).
- [34] Jasper van de Kraats, Kristian K. Nielsen, and Georg M. Bruun, “Holes and magnetic polarons in a triangular lattice antiferromagnet,” *Phys. Rev. B* **106**, 235143 (2022).
- [35] K. Knakkegaard Nielsen, “Exact nonequilibrium hole dynamics, magnetic polarons, and string excitations in antiferromagnetic bethe lattices,” *Phys. Rev. B* **106**, 115144 (2022).
- [36] F. Grusdt, M. Kánasz-Nagy, A. Bohrdt, C. S. Chiu, G. Ji, M. Greiner, D. Greif, and E. Demler, “Parton theory of magnetic polarons: Mesonic resonances and signatures in dynamics,” *Phys. Rev. X* **8**, 011046 (2018).
- [37] Fabian Grusdt, Annabelle Bohrdt, and Eugene Demler, “Microscopic spinon-charge theory of magnetic polarons in the  $t-j$  model,” *Phys. Rev. B* **99**, 224422 (2019).
- [38] A. Bohrdt, Y. Wang, J. Koepsell, M. Kánasz-Nagy, E. Demler, and F. Grusdt, “Dominant fifth-order correlations in doped quantum antiferromagnets,” *Phys. Rev. Lett.* **126**, 026401 (2021).
- [39] Joannis Koepsell, Dominik Bourgund, Pimonpan Sompert, Sarah Hirthe, Annabelle Bohrdt, Yao Wang, Fabian Grusdt, Eugene Demler, Guillaume Salomon, Christian Gross, and Immanuel Bloch, “Microscopic evolution of doped mott insulators from polaronic metal to fermi liquid,” *Science* **374**, 82–86 (2021),

- <https://www.science.org/doi/pdf/10.1126/science.abe7165>.
- [40] D. Pimenov, A. Camacho-Guardian, N. Goldman, P. Massignan, G. M. Bruun, and M. Goldstein, “Topological transport of mobile impurities,” *Phys. Rev. B* **103**, 245106 (2021).
- [41] A. Camacho-Guardian, N. Goldman, P. Massignan, and G. M. Bruun, “Dropping an impurity into a chern insulator: A polaron view on topological matter,” *Phys. Rev. B* **99**, 081105 (2019).
- [42] Li Bing Tan, Ovidiu Cotlet, Andrea Bergschneider, Richard Schmidt, Patrick Back, Yuya Shimazaki, Martin Kroner, and Ata ç İmamoğlu, “Interacting polaron-polaritons,” *Phys. Rev. X* **10**, 021011 (2020).
- [43] A. Camacho-Guardian, M. A. Bastarrachea-Magnani, and G. M. Bruun, “Mediated interactions and photon bound states in an exciton-polariton mixture,” *Phys. Rev. Lett.* **126**, 017401 (2021).
- [44] Li Bing Tan, Oriana K Diessel, Alexander Popert, Richard Schmidt, Atac Imamoglu, and Martin Kroner, “Bose polaron interactions in a cavity-coupled monolayer semiconductor,” arXiv preprint arXiv:2212.11145 (2022).
- [45] Jack B Muir, Jesper Levinsen, Stuart K Earl, Mitchell A Conway, Jared H Cole, Matthias Wurdack, Rishabh Mishra, David J Ing, Eliezer Estrecho, Yuerui Lu, *et al.*, “Interactions between fermi polarons in monolayer ws<sub>2</sub>,” *Nature Communications* **13**, 6164 (2022).
- [46] Jack B Muir, Jesper Levinsen, Stuart K Earl, Mitchell A Conway, Jared H Cole, Matthias Wurdack, Rishabh Mishra, J David, Eliezer Estrecho, Yuerui Lu, *et al.*, “Exciton-polaron interactions in monolayer ws<sub>2</sub>,” arXiv preprint arXiv:2206.12007 (2022).
- [47] SI Mistakidis, GM Koutentakis, GC Katsimiga, Th Busch, and Peter Schmelcher, “Many-body quantum dynamics and induced correlations of bose polarons,” *New Journal of Physics* **22**, 043007 (2020).
- [48] Aleksı Julku, Jami J Kinnunen, Arturo Camacho-Guardian, and Georg M Bruun, “Light-induced topological superconductivity in transition metal dichalcogenide monolayers,” *Physical Review B* **106**, 134510 (2022).
- [49] Arne Brataas, Bart van Wees, Olivier Klein, Grégoire de Loubens, and Michel Viret, “Spin insulatronics,” *Physics Reports* **885**, 1–27 (2020).
- [50] Niklas Rohling, Eirik Løhaugen Fjærbu, and Arne Brataas, “Superconductivity induced by interfacial coupling to magnons,” *Phys. Rev. B* **97**, 115401 (2018).
- [51] Eirik Erlandsen and Asle Sudbø, “Schwinger boson study of superconductivity mediated by antiferromagnetic spin fluctuations,” *Physical Review B* **102**, 214502 (2020).
- [52] Øyvind Johansen, Akashdeep Kamra, Camilo Ulloa, Arne Brataas, and Rembert A Duine, “Magnon-mediated indirect exciton condensation through antiferromagnetic insulators,” *Physical Review Letters* **123**, 167203 (2019).
- [53] Eirik Erlandsen, Akashdeep Kamra, Arne Brataas, and Asle Sudbø, “Enhancement of superconductivity mediated by antiferromagnetic squeezed magnons,” *Physical Review B* **100**, 100503 (2019).
- [54] Eirik Erlandsen, Arne Brataas, and Asle Sudbø, “Magnon-mediated superconductivity on the surface of a topological insulator,” *Physical Review B* **101**, 094503 (2020).
- [55] Henning G Hugdal and Asle Sudbø, “Possible odd-frequency amperian magnon-mediated superconductivity in topological insulator–ferromagnetic insulator bilayer,” *Physical Review B* **102**, 125429 (2020).
- [56] K Bernardet, GG Batrouni, J-L Meunier, Guido Schmid, Matthias Troyer, and A Dorneich, “Analytical and numerical study of hardcore bosons in two dimensions,” *Physical Review B* **65**, 104519 (2002).
- [57] Benjamin Remez and Nigel R. Cooper, “Leaky exciton condensates in transition metal dichalcogenide moiré bilayers,” *Phys. Rev. Res.* **4**, L022042 (2022).
- [58] Aleksı Julku, “Nonlocal interactions and supersolidity of moiré excitons,” *Phys. Rev. B* **106**, 035406 (2022).
- [59] Cheng Chin, Rudolf Grimm, Paul Julienne, and Eite Tiesinga, “Feshbach resonances in ultracold gases,” *Rev. Mod. Phys.* **82**, 1225–1286 (2010).
- [60] Alexander Altland and Ben D Simons, *Condensed matter field theory* (Cambridge university press, 2010).
- [61] H. Heiselberg, C. J. Pethick, H. Smith, and L. Viverit, “Influence of induced interactions on the superfluid transition in dilute fermi gases,” *Phys. Rev. Lett.* **85**, 2418–2421 (2000).
- [62] A. Camacho-Guardian and Georg M. Bruun, “Landau effective interaction between quasiparticles in a bose-einstein condensate,” *Phys. Rev. X* **8**, 031042 (2018).
- [63] Francesco Scazza, Matteo Zaccanti, Pietro Massignan, Meera M Parish, and Jesper Levinsen, “Repulsive fermi and bose polarons in quantum gases,” *Atoms* **10**, 55 (2022).
- [64] VL Berezinskii, “Destruction of long-range order in one-dimensional and two-dimensional systems possessing a continuous symmetry group. ii. quantum systems,” *Sov. Phys. JETP* **34**, 610–616 (1972).
- [65] John Michael Kosterlitz and David James Thouless, “Ordering, metastability and phase transitions in two-dimensional systems,” *Journal of Physics C: Solid State Physics* **6**, 1181 (1973).
- [66] JM Kosterlitz, “The critical properties of the two-dimensional xy model,” *Journal of Physics C: Solid State Physics* **7**, 1046 (1974).
- [67] Shaoyu Yin, J.-P. Martikainen, and P. Törmä, “Fulde-ferrell states and berezinskii-kosterlitz-thouless phase transition in two-dimensional imbalanced fermi gases,” *Phys. Rev. B* **89**, 014507 (2014).
- [68] A Camacho-Guardian and R Paredes, “Superfluidity of a dipolar fermi gas in 2d optical lattices bilayer,” *Annalen der Physik* **528**, 778–784 (2016).
- [69] Dante M. Kennes, Martin Claassen, Lede Xian, Antoine Georges, Andrew J. Millis, James Hone, Cory R. Dean, D. N. Basov, Abhay N. Pasupathy, and Angel Rubio, “Moiréheterostructures as a condensed-matter quantum simulator,” *Nature Physics* **17**, 155–163 (2021).
- [70] Niclas Götting, Frederik Lohof, and Christopher Gies, “Moiré-bose-hubbard model for interlayer excitons in twisted transition metal dichalcogenide heterostructures,” *Physical Review B* **105**, 165419 (2022).
- [71] Hongyi Yu, Gui-Bin Liu, Jianju Tang, Xiaodong Xu, and Wang Yao, “Moiré excitons: From programmable quantum emitter arrays to spin-orbit-coupled artificial lattices,” *Science advances* **3**, e1701696 (2017).
- [72] Fengcheng Wu, Timothy Lovorn, Emanuel Tutuc, and Allan H MacDonald, “Hubbard model physics in transition metal dichalcogenide moiré bands,” *Physical review letters* **121**, 026402 (2018).
- [73] T Lahaye, C Menotti, L Santos, M Lewenstein, and T Pfau, “The physics of dipolar bosonic quantum gases,”

- Reports on Progress in Physics **72**, 126401 (2009).
- [74] Lauriane Chomaz, Igor Ferrier-Barbut, Francesca Ferlaino, Bruno Laburthe-Tolra, Benjamin L Lev, and Tilman Pfau, “Dipolar physics: a review of experiments with magnetic quantum gases,” Reports on Progress in Physics **86**, 026401 (2022).